Scripta METALLURGICA Vol. 18, pp. 515-519, 1984 Pergamon Press Ltd.
Printed in the U.S.A. All rights reserved

ACCURATE CONTRACTION AND CREEP MEASUREMENTS DURING STRUCTURAL RELAXATION OF AMORPHOUS $Fe_{40}Ni_{40}B_{20}$

A.L. Mulder, S. van der Zwaag*, E. Huizer, A. van den Beukel
Laboratory of Metallurgy, Delft University of Technology
Rotterdamseweg 137, 2628 AL Delft, The Netherlands
*AKZO Corporate Research, Arnhem, The Netherlands

(Received January 5, 1984)
(Revised March 5, 1984)

Introduction

Given sufficient atomic mobility metallic glasses can lower their free energy by altering their amorphous structure. This process of structural relaxation occurs during annealing at temperatures well below the glass temperature and is generally considered to consist of two distinct types of relaxation: TSRO and CSRO. In the first type only the topological atomic positions are considered, regardless of the chemical species of the atoms. Changes of these topological positions, e.g., the interatomic distances, are thus described in terms of topological short range order (TSRO). As a result of TSRO the density of the glass will change. In the second type of rearrangement the chemical species of the atoms is taken into account. Consequently chemical or compositional short range order (CSRO) describes changes in the local surroundings of a given atom. It is comparable to order-disorder processes in crystalline materials.

In an as-quenched glass the amount of free volume that is frozen in is high and the degree of short-range order low. Annealing of an as-quenched glass will result in a decrease of the amount of free volume (TSRO) and an increase of the degree of short-range order (CSRO).

A large number of physical properties is affected by structural relaxation and some of them have been measured to study the process of structural relaxation (1). However, in most cases a physical property changes as the result of both CSRO and TSRO, e.g., the electrical resistance (2) and Young's modulus (3). In these studies the contributions of CSRO and TSRO to the relaxation were successfully separated. This would be easier if a physical property can be found which is only affected by CSRO or TSRO. In the literature (4) it is argued that a specimen dimension or density is such a property, which should be affected by TSRO only. Density (5) and length (6-9) measurements have been published in which the occurrence of structural relaxation is demonstrated and from which kinetic parameters were deduced.

In order to test a recently proposed model (10) for the kinetics of structural relaxation accurate length measurements were performed. This paper deals with the experimental technique and some results are presented and compared with the literature. A detailed analysis of the measurements in terms of the model (10) will be presented elsewhere. The question of whether or not the specimen dimensions are affected by CSRO will also be discussed there.

Experimental

Length measurements were performed in an apparatus originally designed for creep and viscosity measurements; it is shown schematically in Fig. 1. An insulated water cooled bell-jar covers the set-up consisting of two quartz rods connected at their top by a fixed traverse. One end of the specimen is mounted on this traverse, the other end is connected to the core of a LVDT (Hewlett-Packard, type 24 DCDT-100). The force on the specimen due to the weight of the core amounts to (5×10^{-2} N). In case of the creep experiments this force was increased to 10.12 N by placing a weight on the core holder.

The coil of the LVDT is mounted on one of the quartz rods and the temperature of the LVDT is kept constant by a water cooled housing. Part of the specimen ($\sim$ 200 mm) is surrounded by a furnace. This furnace consists of a thick-walled copper tube (inner dia. $\emptyset = 6$mm) on which a spirally wound length of thermocoax heating wire is soldered. To compensate for end losses the

0036-9748/84 $3.00 + .00
Copyright (c) 1984 Pergamon Press Ltd.

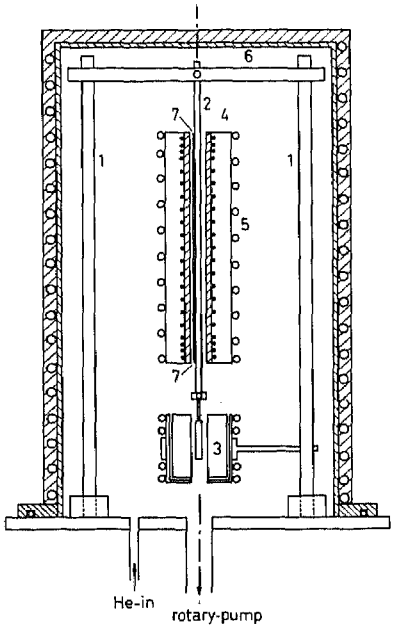

FIG. 1
Schematic drawing of the apparatus used for creep and contraction experiments.
1 = quartz rods
2 = specimen
3 = LVDT (watercooled)
4 = furnace
5 = heat shield (watercooled)
6 = bell-jar (watercooled)
7 = thermocouple
The cooling water circuit is externally stabilized at 303 K.

density of turns is increased at both ends of the furnace. Coaxially with the furnace a water-cooled brass tube (Ø = 60 mm) is placed; it acts as a heat shield for the quartz rods. In order to obtain a homogeneous temperature over the full length of the furnace, "hot spots" were cooled by a number of "heat-leaks". These heat-leaks were obtained by copper wires in contact with both the furnace and the cooled brass tube. By carefully adjusting the number and magnitude of these heat leaks a homogeneous temperature ($\pm$ 0.25 K) was obtained over a length of $\sim$ 180 mm of the specimen. Outside this length the temperature dropped rapidly ($\geq$ 1.5 $K.mm^{-1}$).

Since the temperature profile of the furnace depends very much on the He-pressure inside the bell-jar care was taken to maintain a constant dynamical pressure of 16 Pa He. Due to the construction described above the absolute gauge length l of the specimens is not known but length changes Δl can be measured very accurately. In the calculations of $\Delta l/l$ a value of l = 200 mm was used.

The temperature of the specimen is controlled by a thermocouple (mounted near the specimen inside the bore of the furnace) and a temperature controller (L.I.E., type TTC-1100). This controller can be programmed to yield linear heating of the specimen at various heating rates. For heating rates $\leq$ 1.25 $K.min^{-1}$ the actual temperature $T_{act} = T_{set} \pm 0.05$ K. An externally stabilized cooling water circuit keeps the bell-jar, the heat-shield and the LVDT at a temperature of 303 $\pm$ 0.1 K.

The LVDT signal is measured at time invervals of 1 min or more by a Hewlett-Packard 3450 B multi-function meter in the ratio-mode, thus eliminating instabilities of the 24V power supply of the LVDT. From the measured ratio-values the length changes of the specimen were calculated using a calibration curve obtained by calibrating the LVDT against a dial gauge. Length changes as small as 2.10^{-4} mm could be detected.

All experiments presented here were performed on ribbons of the alloy $Fe_{40}Ni_{40}B_{20}$ (Vitrovac 0040, obtained from Vacuumschmelze) with cross-sectional dimensions of approximately 2.85 x 0.041 mm^2 = 0.115 $\pm$ 0.005 mm^2. Using this value the stress at which the length measurements and the creep experiment were performed were calculated as 0.4 MPa and 88 MPa respectively.

Results

Fig. 2 shows the results of two subsequent linear heating/cooling cycles on an initially as-quenched specimen. Heating was performed at a rate of 1.25 $K.min^{-1}$ up to 623 K immediately followed by cooling down at the same rate. For practical reasons the temperature programmer

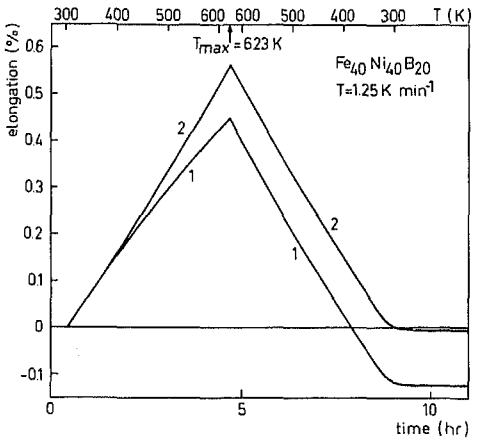

FIG. 2

Elongation during two succesive heating/ cooling cycles. 1 = as-quenched, 2 = second run on the same sample.

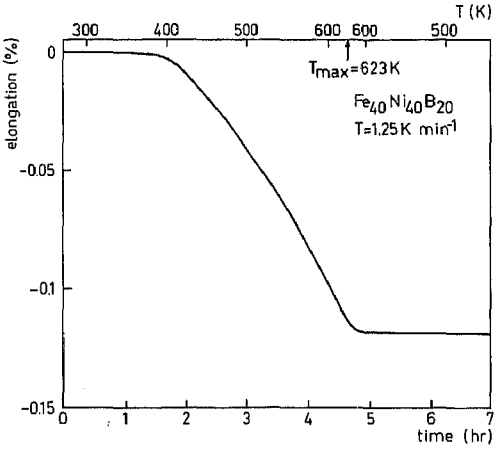

FIG. 3

Contraction during structural relaxation obtained by subtraction of curves 1 and 2 from Fig. 1.

starts (at t=0) and stops at 273 K, which is 30 K below the temperature at which the set-up is stabilized externally. This explains the two horizontal parts of the length vs time plots of Fig. 2. Comparison of the first and second run in Fig. 2 shows that in the first run for an as-quenched specimen a contraction starts beyond $\sim$ 425 K. At the end of the first run to 623 K and back the total contraction amounts to 0.124%. During the second run to the same temperature a much smaller contraction of 0.004% occurs.

The evolution of the contraction as a function of temperature is shown in Fig. 3 in which the difference between run 1 and run 2 from Fig. 2 is plotted. If the contraction during the second run is neglected Fig. 3 represents the effects of structural relaxation on the length of an as-quenched specimen.

Fig. 4 shows the results of an isothermal experiment at 487 K. Heating to this temperature was performed at the same rate of 1.25 K.min^{-1}, and after an isothermal anneal for $\sim$ 60 hr the specimen was cooled down to 303 K again at a rate of $\sim$ 7 K.min^{-1}. At the end of this experiment the total contraction S determined at 303 K was 0.061%. This value is much larger than the isothermal contraction observed at 487 K which amounts to 0.024%. The difference in contraction (0.037%) has occurred during heating to 487 K. From Fig. 3 it is estimated that during heating to 487 K a contraction of 0.036% will occur. The agreement (within 10 ppm) of this value with that obtained from the isothermal experiment indicates the reliability of the measurements.

Fig. 5 shows a number of isothermal contraction curves at different temperatures. The annealing temperatures were reached at a rate of 1.25 K.min^{-1} in the case of 487 K and 523 K. For the curves at 546 K and 578 K a heating rate of $\sim$ 17.5 K.min^{-1} was used. The position of each curve along the vertical axis was determined from the respective value of the total contraction S (including that during linear heating) at the end of each experiment at 303 K.

Creep experiments on specimens which are subjected to structural relaxation will be affected by two effects. The first effect is contraction due to the disappearance of the free volume just described. The second effect that will play a role is the increase of Young's modulus E due to structural relaxation. Fig. 6 shows this increase as an increase of v^2, where v is the longitudinal sound velocity ($E=\rho v^2$). During a creep experiment the elastic strain due to the load will decrease because E increases (3,4). Fig. 7 shows the influence of both effects on the observed creep curve at 546 K under a load of 88 MPa. Curve 1 in Fig. 7 is the observed contraction at 546 K. Curve 2 is the observed creep curve at 546 K under a stress of 88 MPa. If it is assumed that the magnitude and the rate of contraction are not affected by the applied stress, curve 3 in Fig. 7 shows the creep curve corrected for the contraction effect. As the isothermal change of E at 546 K is known (3), curve 3 can be corrected for this E-effect. As a result curve 4 in Fig. 7 is found. Fig. 7 shows that creep results have to be corrected for the two effects of structural relaxation, the contraction and the increase of Young's modulus, and that these corrections are far from negligible.

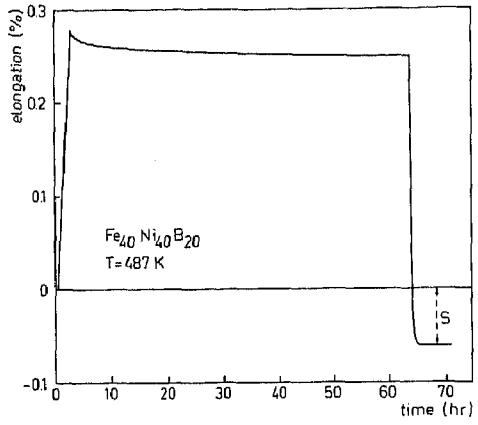

FIG. 4
Elongation during isothermal annealing. S is the total contraction at the end of the experiment.

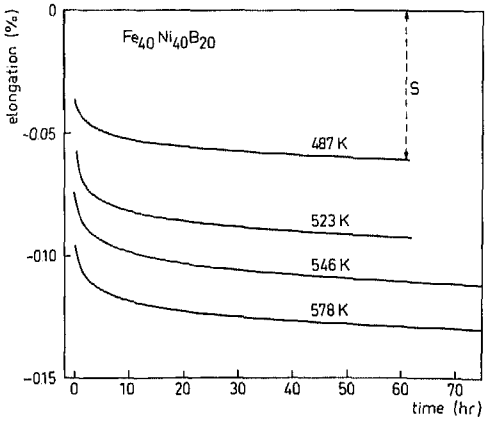

FIG. 5
Isothermal contraction curves at the temperatures indicated. For heating rates see text.

Discussion

Comparing our linear heating results on $Fe_{40}Ni_{40}B_{20}$ with the results of Kursumović, et al. (7) on the same alloy there are two important differences. The first discrepancy concerns the magnitude of the elongation during linear heating at a comparable rate (1.25 $K.min^{-1}$ vs 1.5 $K.min^{-1}$). From the curves of Kursumović, et al. an elongation of 0.26% was estimated at a temperature of 623 K during linear heating of an as-quenched sample. Our measurement (Fig. 2, curve 1) yields ≈ 0.45%.

The second difference is observed in connection with the dilatation minima reported by Kursumović, et al. during linear heating (7) as well as during isothermal annealing (6). These dilatation minima are absent in all our results.

Contrary to the conclusion of Kursumović, et al. (6) that there is a saturation value of the isothermal contraction, our measurements (Fig. 5) do not show any indication of such a saturation. However, the experimental evidence for the supposed saturation value is weak in (6).

Creep curves can be used (11) to calculate the viscosity η of metallic glasses using the expression $\eta = \sigma/3\dot{\varepsilon}$, where σ is the stress and $\dot{\varepsilon}$ the strain rate. It is observed (11) that during structural relaxation the viscosity increases linearly with time and that the rate of increase exhibits an Arrhenius-type temperature dependence. In the existing models (10,11) for structural relaxation $d\eta/dt$ plays an important role. Up to now the experimental values for $d\eta/dt$ were all obtained from creep curves as curve 2 in Fig. 7 without taking into account the effects of the contraction and the increase of Young's modulus. From curve 2 a value of $d\eta/dt = 4.0 \times 10^{10}$ Pa is calculated. If the contraction correction is applied a value of $d\eta/dt = 3.7 \times 10^{10}$ Pa is found and if also a correction is made for the increase of Young's modulus, $d\eta/dt = 3.3 \times 10^{10}$ Pa So at 546 K and 88 MPa a total correction of ∿ 17.5% must be applied to the measured value of $d\eta/dt$ to obtain the correct value.

Experiments at different temperatures and stresses are planned to determine whether the activation energy for $d\eta/dt$ is affected if the contraction due to the disappearance of the free volume and due to the increase of Young's modulus is taken into account. Also the role of the stress on structural relaxation will be investigated, in particular the concept of a threshold stress in relaxation as proposed by Taub (12).

Conclusions

1) Accurate measurements of the contraction of $Fe_{40}Ni_{40}B_{20}$ during structural relaxation do not show dilatation minima.
2) If the contraction and the increase of Young's modulus are taken into account, creep measurements yield lower values for the viscosity and its rate of change than deduced from the observed apparent creep curves.

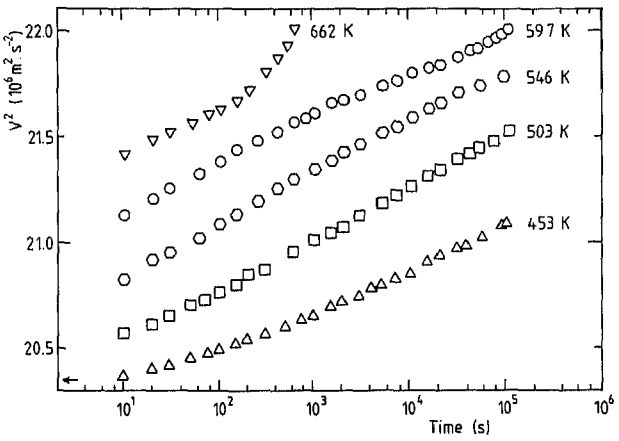

FIG. 6
Isothermal increase of Young's modulus E at various temperatures (3). $E = \rho v^2$, where ρ is the density and v the longitudinal sound velocity. ($\Delta\rho/\rho \ll \Delta v^2/v^2$)

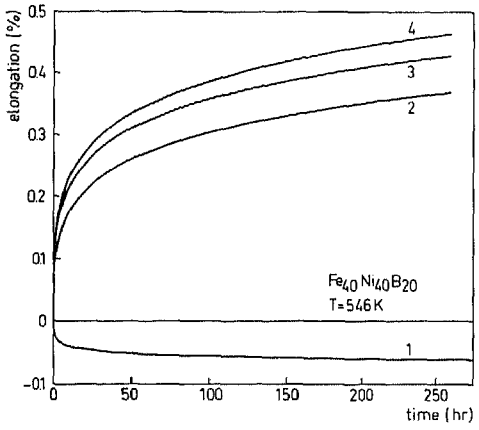

FIG. 7
The effects of structural relaxation on the observed creep curve at 546 K and 88 MPa. 1 = observed contraction curve at 546 K and .4 MPa, 2 = observed creep curve at 546 K and 88 MPa, 3 = calculated creep curve by subtracting curve 1 from curve 2, 4 = calculated creep curve by correction of curve 3 for the increases of E from Fig. 6, 546 K.

References

1. A.L. Greer, LAM-5 Conf. Proc., J. Non-Cryst. Solids, 61 & 62 (1984) 737.
2. M.E. Sonius, B.J. Thijsse, A. van den Beukel, Scripta Met. 17 545 (1983).
3. A.L. Mulder, S. van der Zwaag, A. van den Beukel, LAM-5 Conf. Proc., see ref.1, 979.
4. M.G. Scott, A. Kursumović, Acta Met. 30 853 (1982).
5. H.S. Chen, J. Appl. Phys. 49 3289 (1978).
6. A. Kursumović, R.W. Cahn, M.G. Scott, Scripta Met. 14 1245 (1980).
7. A. Kursumović, E. Girt, E. Babić, B. Leontić, N. Njuković, J. Non-Cryst. Sol. 44 57 (1981).
8. E. Girt, P. Tomić, I. Gazdić, T. Mihać, J. Phys. F: Met. Phys. 13 747 (1983).
9. T. Komatsu, M. Takeuchi, K. Matusita, R. Yokota, J. Non-Cryst. Sol. 57 129 (1983).
10. A. van den Beukel, S. Radelaar, Acta Met. 31 419 (1983).
11. A.I. Taub, F. Spaepen, Acta Met. 28 1781 (1980).
12. A.I. Taub, Acta Met. 30 2129 (1982).